PHYSICAL REVIEW D VOLUME 11, NUMBER 5 1 MARCH 1975

Does the Pomeron have vacuum quantum numbers?

Jon Pumplin*
Department of Physics, Michigan State University, East Lansing, Michigan 48824

G. L. Kane†
Department of Physics, University of Michigan, Ann Arbor, Michigan 48104
(Received 18 November 1974)

From general arguments, the imaginary part of every elastic scattering amplitude at sufficiently large impact parameter is governed by the two-*pion* exchange cut in the t channel. Consequently, the large-impact-parameter tail of the Pomeron is not an SU(3) singlet. We calculate the contribution of the tail (typically about $\frac{1}{4}$ of σ_{tot}) approximately, and thereby predict observable differences between high-energy total cross sections for πp and Kp, and between pp, Λp, Σp, and Ξp. We estimate the asymptotic difference between πp and pp cross sections. We also obtain nonzero estimates for the diffractive helicity-flip component of elastic scattering and for diffractive contributions to processes such as $\pi p \to A_2 p$ and $Kp \to K^*(890)p$. We predict cross sections for A_2 and K^* at Fermilab, and elastic polarizations, e.g., in $pp \to pp$ and $\Lambda p \to \Lambda p$, at asymptotic energies.

I. INTRODUCTION

Total cross sections and elastic scattering at small t are *approximately* constant at very high energy. This indicates a singularity in the crossed-channel angular momentum plane, near $J=1$ at $t=0$. It is called the Pomeron, and is presumed to be related to diffraction scattering.

One expects diffraction scattering to be independent of the isospin projections of the incident particles, and hence expects the Pomeron to have $I=0$. This is confirmed by the observation that πp, Kp, and pp differential cross sections are large compared to their $I=1$ exchange counterparts $\pi^- p \to \pi^0 n$, $K_L p \to K_S p$, and $np \to pn$, which fall with energy like $s^{2\alpha-2}$, where $\alpha \lesssim 0.5$ near $t=0$.

More generally, the Pomeron is often conjectured to have quantum numbers identical to the vacuum, including being a singlet in SU(3). We will present here a theoretical argument that, to the contrary, the Pomeron deviates from being an SU(3) singlet in much the same way that the mass operator does. In fact, the nonsinglet behavior in our theory is caused by the mass splitting. For example, we predict $\sigma_{\pi p} - \sigma_{Kp}$ and $\sigma_{pp} - \sigma_{\Lambda p}$ to remain nonzero at the highest energies.

The total cross section can be expressed as an integral over positive-definite contributions from each impact parameter b. These contributions are proportional to the interaction probability at b, and are given by the Hankel transform of the imaginary part of the nonflip amplitude,

$$\tilde{M}(b) = \frac{1}{2s}\int_{-\infty}^{0} dt\, J_0(b\sqrt{-t})M(t)\,. \qquad (1)$$

This formula is equivalent to the partial-wave series at high energy. $\tilde{M}(b)$ can be extracted from the data by using the approximation $M(t) \simeq (16\pi d\sigma/dt)^{1/2}s$, which neglects spin flip and the real part.

The impact-parameter amplitude $\tilde{M}(b)$ is related to production processes through unitarity. At large impact parameter, say $b \gtrsim 1.5$ F, it must be mainly the "shadow" of production processes which involve pion exchange, since the pion is the lightest hadron, and therefore produces the force of longest range.[1,2] Pictorially, a virtual pion from the "cloud" around one particle interacts with the "cloud" or "core" of the other. These processes generate a two-pion cut in the imaginary part of the elastic amplitude, with threshold behavior $(t-4m_\pi^2)^{\alpha+0.5}$, where $\alpha = \alpha_P(4m_\pi^2) \simeq 1$. This produces

$$\tilde{M}(b) \propto b^{-\alpha-2}e^{-2m_\pi b} \qquad (2)$$

at large b. The exponent in Eq. (2) is determined by the mass in the t channel, and the two-pion state is thereby dominant.

The dependence of the two-pion exchange tail on b is determined by the position and threshold behavior of the branch cut. We have discussed its energy dependence in a previous paper.[2] It will suffice at present to say that it increases rather slowly—e.g., in pp scattering it increases by a few mb between $s=300$ and 3000 GeV^2. The power-law falloff which is associated with pion exchange in exclusive processes, such as charge-exchange scattering, is canceled by the sum over states in unitarity.

Our objective here is to relate the *strengths* of the tails for various observable processes, which include elastic scattering of γ, π, K, p, Λ, Σ, Ξ, on a proton target. The nonsinglet SU(3) character of the Pomeron follows directly from the fact that the SU(3) analogs of the 2π state in the t channel, e.g., $K\bar{K}$, are suppressed at large b because of their much larger mass. At small b, all contributions are suppressed by unitarity, so that contributions from $K\bar{K}$ cannot be enhanced there. The theory can be tested directly by observing the nonexponential shape of $d\sigma/dt$ for $|t| \lesssim 0.2\ \mathrm{GeV}^2$, which is sensitive to the strength of the two-pion cut.

Our model also provides an estimate of the large-impact-parameter contribution to *helicity flip* in elastic scattering, and to *inelastic processes* such as $\pi p \to A_2 p$, $Kp \to K^*(890)p$. The model is interesting from a theoretical point of view, in that it displays convincing mechanism whereby *diffractive* contributions to these processes are nonzero. The model further leads to numerical estimates, which suggest that the diffractive contributions to these processes will come into view, via their energy dependence, at Fermilab energies. The numerical estimates for inelastic processes are somewhat less certain than for the nonflip elastic amplitude, because only in the latter case does unitarity require $\tilde{M}(b)$ to be positive definite, so that cancellations cannot occur from small b.

II. THE MODEL

In this section we describe a method for calculating the strength of the two-pion exchange tail in various physical processes. The method entails estimating the coefficient of the asymptotic form (2), and then assuming that form to hold down to $b \simeq 1$ F. This procedure is somewhat crude, but nevertheless useful, in that it reveals the approximate dependence of the two-pion effect on masses and coupling constants, and also confirms that the estimates which we obtain phenomenologically are of reasonable magnitude.

The majority of the amplitude at large impact parameter is generated by pion exchange processes which involve a *low-mass* system at one end of the exchange.[2] The importance of low mass will become apparent shortly. The contribution of these processes to the imaginary part of the elastic amplitude is represented by Fig. 1. This diagram, in which particle a can be said to dissociate into $\pi + c$, implies the loop integral

$$M_a(s,t) = \frac{g^2}{16\pi^3} \int \frac{d^3q M_{\pi p}(s',t)}{q_0[(k-q)^2 - m_\pi{}^2][(k'-q)^2 - m_\pi{}^2]} \tag{3}$$

M_a and $M_{\pi p}$ refer to s-channel absorptive, i.e., imaginary, parts. Further dissociations, with their corresponding two-pion cuts, are implicit in the internal amplitude $M_{\pi p}$. We do not need to consider cut terms generated by dissociation of the proton, if they do not also involve dissociation of particle a, because our interest here is in *differences* between various particles a. The modifications to (3) required by spin and isospin will be discussed shortly.

Our present objective is to calculate the Hankel transform (1) of Eq. (3) in the limit of large b. We will then use the asymptotic form down to $b \sim 1$ F in order to estimate the contribution of the tail to the total cross section. The correctness of this procedure can be checked by direct numerical integration of Eqs. (1) and (3), which we discuss at the end of this section.

The discontinuity across the two-pion exchange cut in Eq. (3) is an absorptive part in both s and t. It is equivalent to the Mandelstam double-spectral function for the box diagram, integrated over the mass of one side of the box. By means of the standard Feynman parametrization method, we rewrite (3) as a dispersion integral in t:

$$\begin{aligned} M_a(s,t) &= \frac{g^2}{16\pi^2\sqrt{s}} \int \frac{ds'}{Q} M_{\pi p}(s't) \int_{t_0}^{\infty} \frac{dt'}{(t'-t)[t'(t'-t_0)]^{1/2}}\,, \\ s' &= (k+p-q)^2\,, \\ Q &= [s^2 - 2s(s'+m_c{}^2) + (s'-m_c{}^2)]^{1/2}/2\sqrt{s}\,, \\ t_0 &= \{m_\pi{}^2 s^2 + s[m_\pi{}^4 - m_\pi{}^2(s'+m_c{}^2+2m_a{}^2) + (s'-m_a{}^2)(m_c{}^2-m_a{}^2)] + m_a{}^2(s'-m_c{}^2)^2\}/Q^2 s\,. \end{aligned} \tag{4}$$

Assuming as an approximation that $M_{\pi p}(s',t) = s'f(t)$, which corresponds to a constant πp differential cross section, and letting $s \to \infty$ with $s' = (1-x)s$, we obtain

$$M_a(s,t) = \frac{g^2}{8\pi^2} M_{\pi p}(s,t) \int_0^1 dx \frac{1-x}{x} \int_{t_0}^{\infty} \frac{dt'}{(t'-t)[t'(t'-t_0)]^{1/2}}\,, \tag{5}$$

$$t_0 = \frac{4}{x^2}[x m_\pi{}^2 + (1-x)m_c{}^2 - x(1-x)m_a{}^2]\,. \tag{6}$$

The integration variable x is the fraction of a's momentum which is carried by c in the lab, or center of mass, frame. t_0 is close to its minimum value of $4m_\pi^2$ only when x is close to 1. Therefore, only $x \simeq 1$ contributes to the cut near the branch point at $4m_\pi^2$. Thus the total cross section at large b is generated by inclusive production of the low-mass system c in the fragmentation region $x \gtrsim 0.9$. To determine the behavior of the cut in this region, we neglect terms of order $(1-x)^2$ in (5) and (6), and interchange the order of integration to obtain

$$M_a(s,t) \simeq \frac{g^2}{96\pi^2 \tilde{m}^4} M_{\pi p}(s,t) \int_{4m_\pi^2} \frac{dt'(t'-m_\pi^2)^{3/2}}{(t'-t)\sqrt{t'}}\,,$$

$$\tilde{m}^2 = m_c^2 + m_\pi^2 - m_a^2\,. \quad (7)$$

This result displays the discontinuity in t, and is valid when $4m_\pi^2 < t' \lesssim 4(m_\pi^2 + \tilde{m}^2)$, which determines the upper limit of the integral. This region of validity is reasonably large on the scale of m_π^2, except in applications where $m_a \simeq m_c$, which are discussed separately in the Appendix. As $t' \to \infty$, the true discontinuity probably oscillates, in a manner which depends on off-shell effects. We ignore these effects, as an approximation, since we are interested in the region near $4m_\pi^2$, which governs large b.

To calculate the behavior at large b, we approximate $M_{\pi p}(s,t)$ by its value at an average $t=\bar{t}$, and use (1):

$$\tilde{M}_a(s,b) \simeq (g^2/96\pi^2\tilde{m}^4) M_{\pi p}(s,\bar{t}) \times \int_{4m_\pi^2} dt\,(t-4m_\pi^2)^{3/2} t^{-1/2} K_0(b\sqrt{t})\,. \quad (8)$$

Using the asymptotic form of the Bessel function K_0, we find the behavior

$$\tilde{M}_a(s,b) \simeq \frac{g^2 m_\pi^4}{16\pi s \tilde{m}^4} M_{\pi p}(s,\bar{t}) \times \exp(-2m_\pi b)/(m_\pi b)^3 \quad (9)$$

at large b.

This exhibits the asymptotic behavior claimed in Eq. (2), with $\alpha = 1$ because we assumed an energy-independent cross section as an approximation. Our normalization is defined by $\sigma_{\text{tot}} = M(s,0)/s$. Total absorption (the center of the partial-wave unitarity circle) corresponds to $\tilde{M}(s,b) = 4\pi$.

In order to estimate the absolute contribution of the two-pion tail to the total cross section, we approximate $M_{\pi p}(s,\bar{t})$ by $M_{\pi p}(s,0)\exp(A\bar{t}/2)$. Assuming a πp slope $A = 10\ \text{GeV}^{-2}$ and $\bar{t} = 10 m_\pi^2$, we have $M_{\pi p}(s,\bar{t}) \simeq 2.65 s\sigma_{\pi p}$. Note that we require $M_{\pi p}(s,t)$ at the unphysical point $t=\bar{t}$ only because of our method for estimating the Hankel transform

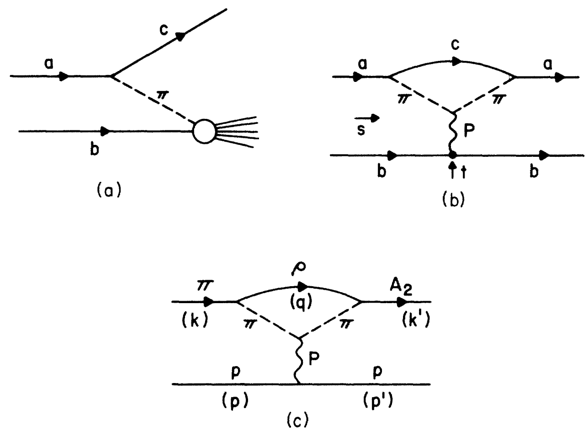

FIG. 1. (a) Particle production by a collision involving a long-range pion. The kinematic region of interest is where the particle or system c has small transverse momentum and large longitudinal momentum, e.g., $x = p_c^{\parallel}/p_a^{\parallel} \simeq 0.9$. (b) The elastic amplitude (absorptive part) which arises from (a) according to unitarity, in triple-Regge notation. This amplitude has the two-pion exchange branch point at $t \simeq 4m_\pi^2$. At $t=0$, it is simply the total cross section associated with (a), by the optical theorem. (c) Two-pion cut contribution to a typical inelastic (diffraction-dissociation) process. Momentum labels are also shown.

of Eq. (7). The actual process under discussion (Fig. 1) involves only physical $t<0$. We integrate the asymptotic form for $b > 0.9$ F, and obtain the result that if

$$\tilde{M}_a(s,b) = N\exp(-2m_\pi b)/(m_\pi b)^3 \quad (10a)$$

then

$$\sigma_a = \int_{0.9\,\text{F}}^{\infty} \tilde{M}_a(s,b)\, b\, db = 3.3N\ \text{mb}\,. \quad (10b)$$

We now obtain an estimate of the large-impact-parameter cross section associated with Fig. 1, or Eq. (3), by combining Eqs. (9) and (10):

$$\sigma_a \simeq g^2 \sigma_{\pi p}(m_c^2 + m_\pi^2 - m_a^2)^{-2} \times (0.00017\ \text{GeV}^2)\,. \quad (11)$$

This equation can be used to make a crude estimate of the tail contribution to any process. For example, a typical value of the strong-interaction coupling constant would be $g^2/4\pi \sim 5\ \text{GeV}^2$. For low-mass states m_c, one has typically $m_c^2 + m_\pi^2 - m_a^2 \sim 0.6\ \text{GeV}^2$. Therefore, $\sigma_a \sim 0.8$ mb. For a high-mass state it is convenient to relate g^2 to a decay width. Assuming particle c to have spin 0, for simplicity, and neglecting the pion mass, we have $g^2 = 16\pi m_c^3 \Gamma_{c\to a\pi}/(m_c^2 - m_a^2)$. Therefore, $\sigma_a \propto \Gamma_{c\to a\pi} m_c^3/(m_c^2 - m_a^2)^3$. This demonstrates that states with large m_c will contribute little to the tail.

We have verified the above estimate by numerically integrating Eqs. (3) and (1) after inserting "form factors"

$$\exp\{C[(k-q)^2+m_\pi^2]\}\exp\{C[(k'-q)^2-m_\pi^2]\}$$

into (3) to suppress the far-off-shell part of the pion propagator. In the case $a=\pi$, $c=\rho$, for example, with appropriate factors for spin and isospin included, as described in Sec. III, the result agrees with Eq. (9) for $b\sim 3$ F, for all reasonable values of C, e.g., $1-4\ \mathrm{GeV}^{-2}$. It lies higher by as much as a factor of 4 for $b\sim 2$ F, and below by a factor of 2 at $b\sim 0.9$ F. These errors tend to compensate each other, so that the estimate of the cross section given in Eq. (11) is about right. We therefore believe our estimate of the cross section associated with the tail to be accurate to within a factor of 2–3.

This uncertainty is not a serious problem at the moment, since we wish to compare the *relative* strengths of the tails for different processes. The ratios among σ_a for various processes should be given fairly accurately by the asymptotic forms. The absolute magnitude for one process can then be determined from experiment.

III. TOTAL CROSS-SECTION DIFFERENCES

In each specific application, we must include additional factors to account for spin and isospin. This chore may be simplified by evaluating the spin factors at $t=4m_\pi^2$, with the pions on the mass shell: $(k-q)^2=(k'-q)^2=m_\pi^2$. The discontinuity near $t=4m_\pi^2$, and hence the behavior at large b, will be unaffected by this approximation.

Let us first consider $a=\pi$ and $c=\rho$ in Fig. 1. Because of the spin of the ρ, Eq. (3) acquires a factor $4(-k\cdot k'+k\cdot qk'\cdot q/m_c^2)$, which we can replace by

$$4m_\pi^2+(m_\pi^2+m_c^2-m_a^2)^2/m_c^2=4m_\pi^2+m_\rho^2\,.$$

It also acquires a factor of 2 due to isospin, since two charge states of the ρ are possible for each charge state of the incident pion. With these factors, Eq. (11) yields $\sigma_\pi=0.69$ mb. (We use $\sigma_{\pi p}=30$ mb, and obtain $g^2/4\pi=2.81$ from the measured ρ width of 146 MeV.)

The result $\sigma_\pi=0.69$ mb is an estimate of the large-b part of $\sigma_{\pi p}$ which comes from the dissociation $\pi\to\rho\pi$. As a test of the plausibility of this result, we note that the Deck model[3] for diffractive dissociation predicts an integrated cross section for $\pi p\to\rho\pi p$ which is similar to Fig. 1, except for a factor $\sigma_{\mathrm{el}}(\pi p)/\sigma_{\mathrm{tot}}(\pi p)\simeq 0.14$. This factor arises because the Deck effect requires elastic scattering of the virtual pion. The diffractive cross section for $\pi^-p\to\pi^-\rho^0p$ is $\simeq 0.2$ mb. With the $\pi^0\rho^-$ state, this leads to an estimate of $(2)(0.2)/0.14=3$ mb for Fig. 1. This estimate includes contributions from all impact parameters, and shows that our result of 0.69 mb for the tail at large b is reasonable, but could be too small by up to a factor of ~ 2.

Now consider the SU(3)-analogous situation where $a=K$ and $c=K^*(890)$. Using Eq. (11) and the appropriate spin and isospin factors, we obtain $\sigma_K=0.23$ mb. Thus we predict $\sigma_{\pi p}-\sigma_{Kp}\simeq 0.5$ mb as a result of the two-pion cut from meson dissociation. States other than ρ/K^* in the role of c could increase this value somewhat, even though they are suppressed by the factor $(m_c^2+m_\pi^2-m_a^2)^{-2}$. The presence of a 2π cut in the internal elastic scattering, which we have ignored, will also tend to increase it.

A further effect which will increase the tail contributions to σ_π, σ_K, and $\sigma_\pi-\sigma_K$ is the dissociation of the nucleon. We estimate this effect crudely as follows: The tail in pp scattering for $b>1$ F amounts to $\simeq 10$ mb.[4] This corresponds to 5 mb from dissociation of each nucleon, if we ignore the small effect of double dissociation. The tail in σ_{Kp} due to nucleon dissociation should therefore be $\simeq(5\ \mathrm{mb})\sigma_{\pi K}/\sigma_{\pi p}$. We estimate this as $\simeq(5\ \mathrm{mb})\sigma_{Kp}/\sigma_{pp}\simeq 2.4$ mb, by using factorization[5] and evaluating σ_{Kp} and σ_{pp} at a lab momentum ~ 20 GeV/c. This momentum is relevant to the tail in σ_{Kp} at ~ 200 GeV/c, because the elastic scattering in Fig. 1 takes place at an invariant energy squared of $(1-x)s\sim s/10$. The corresponding contribution to $\sigma_{\pi p}$ is $(5\ \mathrm{mb})\sigma_{\pi\pi}/\sigma_{\pi p}\simeq(5\ \mathrm{mb})\sigma_{\pi p}/\sigma_{pp}\simeq 3.1$ mb. Adding this effect to the previous ones, *we anticipate diffractive contributions to* $\sigma_{\pi p}-\sigma_{Kp}$ *on the order of* 1.5–2 *mb*. This is smaller than the measured value, which is ~ 3.7 mb at 200 GeV/c (see Ref. 6) if one averages over $\pi^\pm$ and $K^\pm$. The measured value, however, includes contributions from lower-lying vector-meson exchanges. A full analysis of the energy dependence is needed to extract the Pomeron part of the measurement.

The ratio of the tail contributions due to the dissociations $(K\to K^*\pi)/(\pi\to\rho\pi)$ is $\sigma_K/\sigma_\pi=0.34$. This ratio is quite insensitive to our assumptions for estimating the absolute values of σ_K and σ_π. It is very close to the value $\frac{1}{3}$ which would result from assuming exact SU(3) invariance everywhere, except in the requirement that only the two-pion state appears in the t channel. This is because the factor $(m_c^2+m_\pi^2-m_a^2)^{-2}$ and the factor $4m_\pi^2+(m_c^2+m_\pi^2-m_a^2)^2/m_c^2$ which comes from spin are about equal for $a=\pi$, $c=\rho$, and $a=K$, $c=K^*$. At the same time, the ratio of coupling constants $g_{\rho\pi\pi}/g_{K^*K\pi}$ determined from the measured widths of ρ and K^* are close to the pure SU(3) prediction.[7] Our theory thus predicts $\sigma_{\pi p} > \sigma_{Kp}$ in a natural way, based on the fact that the SU(3) coupling $\pi\pi 8$ is larger than $K\pi 8$ by a factor of $\sqrt{3}$, where 8 stands for the octet of vector mesons. Hence the pion cloud amplitude of π is stronger than that of K. The breaking of SU(3) in the cross section occurs because of the breaking in masses— specifically, the small pion mass, which makes dissociations involving pions dominate at large b.

Now let us consider the case where the incident particle a in Fig. 1 is one of the $\frac{1}{2}^+$ baryons N, Λ, Σ, Ξ. In the role of c, we include the $\frac{1}{2}^+$ and $\frac{3}{2}^+$ baryons. States of higher mass will be less important because of the factor $(m_c^2 + m_\pi^2 - m_a^2)^{-2}$, as discussed previously. Thus we have $a = N$, $c = N$, Δ; $a = \Lambda$, $c = \Sigma$, $Y^*(1385)$; $a = \Sigma$, $c = \Lambda$, Σ, Y^*; and $a = \Xi$, $c = \Xi$, $\Xi^*(1530)$. First consider the $\frac{1}{2}^+$ intermediate states. Equation (11) must be modified because $m_c \simeq m_a$, as shown in the Appendix. We find a mass dependence $\propto m_c^{-2}$. The cross section associated with the tail when $a = N$ and $c = N$ is $\sigma_N^{(1/2)} \simeq 4$ mb. Using SU(3) with $f = 0.4$ and $d = 0.6$ to relate the coupling constants, and taking proper account of isospin, we predict

$$\sigma_\Lambda^{(1/2)}/\sigma_N^{(1/2)} = \tfrac{4}{3} d^2 m_p^2/m_\Sigma^2 = 0.30\,,$$

$$\sigma_\Sigma^{(1/2)}/\sigma_N^{(1/2)} = \tfrac{8}{3} f^2 m_p^2/m_\Sigma^2 + \tfrac{4}{9} d^2 m_p^2/m_\Lambda^2 = 0.38\,,$$

and

$$\sigma_\Xi^{(1/2)}/\sigma_N^{(1/2)} = (f-d)^2 m_p^2/m_\Xi^2 = 0.02\,.$$

These ratios are determined mainly by the coupling constants, and are therefore insensitive to the approximations used in estimating the absolute value $\sigma_N^{(1/2)} \simeq 4$ mb. Now consider the $\frac{3}{2}^+$ states for c. We estimate $\sigma_N^{(3/2)} \simeq 2$ mb by numerical integration. We determine the coupling constants for $\pi N\Delta$, $\pi\Lambda Y^*$, $\pi\Sigma Y^*$, and $\pi\Xi\Xi^*$ from the measured widths of the resonances. This is essentially equivalent to obtaining them from SU(3), since SU(3) is known to work well for the $\frac{3}{2}^+$ decays, when the natural phase-space factors are included.[7] We find $\sigma_\Lambda^{(3/2)}/\sigma_N^{(3/2)} = 0.58$, $\sigma_\Sigma^{(3/2)}/\sigma_N^{(3/2)} = 0.18$, and $\sigma_\Xi^{(3/2)}/\sigma_N^{(3/2)} = 0.16$.

Combining the $\frac{1}{2}^+$ and $\frac{3}{2}^+$ results, we predict $\sigma_{pp} - \sigma_{\Lambda p} \simeq 3.6$ mb, $\sigma_{pp} - \sigma_{\Sigma p} \sim 4.1$ mb, $\sigma_{pp} - \sigma_{\Xi p} \simeq 5.6$ mb. These numbers are somewhat crude, but illustrate the direction and approximate size of the total cross-section differences which are to be expected.

Using the impact-parameter projection of Miettinen,[4] we find the pp cross section at $s = 1000$ GeV^2 to be ~ 20 mb for $b > 0.8$ F, and ~ 4 mb for $b > 1.6$ F. Our estimate of ~ 6 mb for the contribution of the two-pion cut due to dissociation of *one* of the protons appears reasonable in the light of these numbers.

The above estimates imply that the two-pion contribution to σ_{pp} is larger than the contribution to $\sigma_{\pi p}$. The two-pion cut therefore produces an asymptotic difference between baryon-baryon and meson-baryon cross sections. If we speculate, for example, that the small-impact-parameter cross sections become equal at extremely high energy, then $\sigma_{pp}/\sigma_{\pi p} \to 1.12$. This ratio is significantly different from 1, although it is considerably smaller than the data at $s \simeq 400$ GeV^2.[6]

IV. SPIN-FLIP PROCESSES

The process in Fig. 1 also implies peripheral contributions to elastic scattering with helicity flip (e.g., $c = \Delta$, with flip coupling at one $\pi N\Delta$ vertex and nonflip at the other). These contributions have the same energy dependence as the nonflip ones. Therefore, on theoretical grounds, we predict that *the Pomeron does not conserve s-channel helicity.*

The asymptotic behavior (2) also holds for helicity-flip amplitudes. In order to discuss the magnitude of the flip amplitude, it is therefore convenient to consider the ratio of flip to nonflip at large b. In pp scattering, we find a ratio of $\simeq 0.7$ for $c =$ nucleon by numerical integration. An approximate calculation of this ratio is given in the Appendix. A similar ratio holds for $c = \Delta$, so we obtain $\tilde{M}_{+-}(b)/\tilde{M}_{++}(b) \simeq 0.35$ at large b. A factor of $\frac{1}{2}$ is included in this ratio, because dissociation of either proton will contribute to M_{++}.

We neglect the spin of the proton which does not dissociate, so M_{+-} means $M_{\frac{1}{2}\frac{1}{2}-\frac{1}{2}\frac{1}{2}}$ or $M_{\frac{1}{2}-\frac{1}{2}-\frac{1}{2}-\frac{1}{2}}$ in the usual helicity amplitude notation. The two-pion cut generated by dissociation of *both* protons in pp scattering would contribute to double-flip amplitudes, including $M_{\frac{1}{2}\frac{1}{2}-\frac{1}{2}-\frac{1}{2}}$ which has $n = 0$, and is therefore nonzero at $t = 0$. This double dissociation effect involves $\pi\pi$ scattering and two dissociations, and will therefore be quite small— probably about 0.04 times the nonflip Pomeron. This is relevant to the validity of high-energy Coulomb interference experiments.

According to our model, $M_{+-} = -M_{-+}$, while $M_{++} = M_{--}$. This is evidence that, when the two-pion tail is added, the Pomeron still has *natural parity*. This result is also true for inelastic diffractive processes, which are discussed in Sec. V.

Because the Pomeron contributes to helicity-flip amplitudes, via the two-pion cut, and because significant real parts away from $t=0$ are implied by the observed energy dependence of $d\sigma/dt$, via dispersion relations,[8] we predict *polarization effects in elastic scattering* to persist to very high energy. To estimate the polarization in pp scattering, we use

$$M_{++}=is11.5Re^{2.21t}J_1(R\sqrt{-t})/\sqrt{-t}$$
$$+is1.94r^2e^{3.93t}J_0(r\sqrt{-t}),$$
$$R^2=8.47+0.33(\ln s-i\pi/2),$$
$$r^2=2.92(\ln s-i\pi/2) \qquad (12)$$

in units where GeV = 1. This formula approximates the measurements of σ_{tot} and $d\sigma/dt$ at CERN ISR. The first term is central in impact parameter, with a radius which expands extremely slowly with s. The second term is peripheral in impact parameter, and we assume it to correspond to the two-pion tail. Without the exponential factors, the first term would be a grey disk of radius R, and the second a δ function at $b=r$. Real parts are generated by the $-i\pi/2$ terms, which are associated with $\ln s$. This association comes from crossing symmetry and analyticity—just as in the case of an even-signature Regge pole, for which

$$[1+\exp(-i\pi\alpha)]s^{\alpha}\propto\exp[\alpha(\ln s-\tfrac{1}{2}i\pi)].$$

For the flip amplitude, we assume

$$M_{+-}=isC1.94r^2e^{3.93t}J_1(r\sqrt{-t}), \qquad (13)$$

which is peripheral in impact parameter. Without the $\exp(3.93t)$ factor, it would correspond to a δ function at $b=r$. We set $C=0.35$, our predicted flip/nonflip ratio at large b. This leads to $M_{+-}/M_{++}\simeq 0.016(\ln s)^{3/2}\sqrt{-t}$ near $t=0$. The resulting polarization, $P=2\,\mathrm{Im}(M_{++}M_{+-}^*)/(|M_{++}|^2+|M_{+-}|^2)$, is shown in Fig. 2. The change in sign of P is associated with a zero in $\mathrm{Re}M_{+-}$. It follows from the expanding peripheral nature of the flip amplitude, and is therefore a rather general prediction. The effect of assuming a slower growth of M_{+-}, by including a factor $\ln(500)/(\ln s-i\pi/2)$ in Eq. (13), is also shown. With this assumption, the zero in P moves to very small $-t$. Our model also predicts a definite overall sign for the polarization (which may correspond to the sign shown in Fig. 2).

The two-pion cut effect for Λ dissociation is smaller than for N by $\simeq 0.4$. We therefore predict a Λ polarization in $\Lambda p\to\Lambda p$ which is similar in shape to Fig. 2, but smaller by a factor of 2–3.

V. INELASTIC PROCESSES

The mechanism of Fig. 1 also leads to diffractive production of inelastic states, i.e., diffraction dissociation. This includes spin-parity changes $0^-\to1^-$ and $0^-\to2^+$. For instance, we can have $a=K$, $a'=c=K^*(892)$, or $a=\pi$, $c=\rho$, and $a'=A_2$. Therefore, *the Pomeron will not respect "Morrison's rule"* because of the two-pion cut, if for no other reason.

To estimate the diffractive production of $K^*(892)$, we use $c=K^*(892)$ and obtain the $K^*K^*\pi$ coupling constant from the width of $\omega\to\pi^0\gamma$, using SU(3) and vector-meson dominance. We calculate the loop integral numerically, including appropriate spin and isospin factors, and form factors as discussed in Sec. III. The result is again rather insensitive to the choice of form factors. The produced K^* has helicity ±1 only. This indicates that our Pomeron is purely natural parity in the t channel, which forbids helicity zero. We find $\tilde{M}(b)\simeq 0.15\exp(-2m_\pi b)/(m_\pi b)^3$ at large b. Extrapolating to small b in a way which makes the amplitude small for $b<0.9$ F, and integrating the cross section over t, we predict $\sigma\simeq 1\ \mu$b for diffractive $Kp\to K^*(892)p$. At low energy, this reaction is dominated by vector-meson and pion exchange. At energies above 100 GeV, the interference term between the diffractive contribution and the ordinary Regge exchange should become visible in the energy dependence. If standard duality arguments hold for vector-meson production, the Reggeon contribution to $K^-p\to K^{*-}p$ has a rotating phase while $K^+p\to K^{*+}p$ is mainly real. The diffractive contribution is mainly imaginary, and will therefore interfere more strongly in the former reaction than in the latter. The sign of the interference term, which determines which cross section is larger, is hard to predict, but would

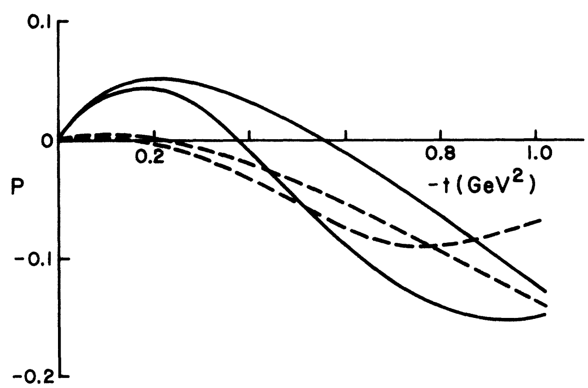

FIG. 2. Predicted polarization in pp scattering. The solid curves correspond to Eqs. (12) and (13) at $s=200$ GeV^2 (upper curve at $t=-0.4$ GeV^2) and $s=2800$ GeV^2. The dashed curves correspond to a slower rise of M_{+-} with s, as described in the text. The energies are again $s=200$ (upper at $t=-0.4$ GeV^2) and 2800 GeV^2.

nevertheless be worthwhile to measure.

We also estimate the diffractive contribution to $\pi p \to A_2 p$, by numerical integration of the triangle diagram [Fig. 1(c)]. We use $c=\rho$, and obtain the necessary coupling constants from the widths of ρ and A_2. Because of the masses of these particles, the two-pion cut actually starts at $t \simeq 1.6 m_\pi^2$ instead of $4m_\pi^2$ (anomolous threshold). The asymptotic behavior (2) is correspondingly modified. The integration of Eq. (3) is complicated by the fact that one of the internal pions in Fig. 1 can be on the mass shell, which generates an extra real part in the final amplitude. Our predicted cross section is $\sim 1-2\ \mu$b.[9] The ratio of helicity-2 to helicity-1 A_2 is $\tilde{M}_2(b)/\tilde{M}_1(b) \simeq 1.5-2$. This leads to $M_2(t)/M_1(t) \sim (2\ \text{GeV}^{-1})\sqrt{-t}$ near $t=0$. The measured A_2 production is $\sigma \simeq 18\ \mu$b at 40 GeV/c.[10] This should correspond to

$$\sigma_{\text{Regge}} + \sigma_{\text{diff}} + 2(\sigma_{\text{Regge}}\sigma_{\text{diff}})^{1/2}\cos\phi\,.$$

The relative phase factor, $\cos\phi$, will be close to 1; so $\sigma_{\text{diff}} \simeq 1.5\ \mu$b implies $\sigma_{\text{Regge}} \simeq 9.1\ \mu$b. The ratio of amplitudes is then $(\sigma_{\text{diff}}/\sigma_{\text{Regge}})^{1/2} \sim 0.3$ at 40 GeV/c. Assuming an energy dependence σ_{diff} = constant, while $\sigma_{\text{Regge}} \propto 1/p_{\text{lab}}$, we predict $\sigma \sim 7\ \mu$b at $p_{\text{lab}} = 200$ GeV. The actual cross section is likely to be somewhat larger because σ_{diff} will increase slowly with s.

VI. CONCLUSION

We have given a serious theoretical argument for the existence of diffractive production of helicity-flip amplitudes, including production of resonances such as K^* and A_2, and for sizable SU(3) nonsinglet diffractive contributions. All of these follow from the same mechanism as the large-impact-parameter tail, which manifests itself in the small-t slope increase in pp scattering at the ISR. That mechanism is the long-range tail in impact parameter, which is due to the two-pion t-channel threshold. The basic physics is very simple, although numerical estimates are model-dependent. A large number of predictions for high-energy cross sections and polarizations are testable, and will provide checks on the estimation procedures and ideas. Because of its effects at small t and high energy, the large-b tail has a surprisingly large effect on interesting observables in high-energy physics.

APPENDIX

When particles a and c in Fig. 1 are both nucleons, the approximations leading from Eqs. (5) and (6) to Eq. (9) break down because $m_a \simeq m_c$. In this case, we proceed as follows. Including the spin of the nucleons introduces a factor $V_{\lambda'\lambda} = \bar{u}^{(\lambda')}(k')(m_c + i\gamma\cdot q)u^{(\lambda)}(k)$ into Eq. (3). By Lorentz invariance and the symmetry of the integrand, we can replace q in this expression by $(k+k')A + (k+p)B/s$. Evaluating A and B at the pion poles, $(k-p)^2 - m_\pi^2 = (k'-p)^2 - m_\pi^2 = 0$, and taking the limit of large s, we obtain $A = x/2$ and $B = 2m_c^2(1-x) - m_\pi^2 + tx/2 \simeq 2m_c^2(1-x)$. Hence $V_{\frac12\frac12} \simeq xt/2 - m_\pi^2$ and $V_{\frac12-\frac12} \simeq (1-x)m_c(-t)^{1/2}$. Over most of the important region of x, we can replace Eq. (6) by $t_0 \simeq 4[m_\pi^2 + (1-x)^2 m_c^2]$. Then Eq. (5) yields

$$M_a^{(\frac12\frac12)}(s,t) \simeq \frac{g^2}{64\pi^2 m_c^2} M_{\pi p}(s,t) \times \int_{4m_\pi^2} \frac{dt'(t'-4m_\pi^2)^{3/2}}{(t'-t)\sqrt{t'}} \tag{A1}$$

for the nonflip amplitude ($V_{\frac12\frac12}$ included). Comparing this with Eqs. (7) and (11), we obtain

$$\sigma_a = g^2 \sigma_{\pi p} m_c^{-2} \times (0.00026\ \text{GeV}^2)\,, \tag{A2}$$

which is analogous to Eq. (11). Using the standard pion-nucleon coupling, $g^2/4\pi = 15$, and including a factor of 3 from isospin, we obtain $\sigma_a = 5.0$ mb for the contribution of Fig. 1 to σ_{pp}. Dissociation of the target proton would add another 5.0 mb. This agrees reasonably well with results obtained by numerical integration. Equations (A1) and (A2) also hold for the SU(3) analogs of the nucleon, e.g., $a=\Lambda$, $c=\Sigma$, or $a=c=\Xi$.

For the flip amplitude, we include $V_{\frac12-\frac12}$ instead, and obtain

$$M_a^{(\frac12-\frac12)}(s,t) \simeq \frac{g^2\sqrt{-t}}{256\pi m_c^2} M_{\pi p}(s,t) \times \int_{4m_\pi^2} \frac{dt'(t'-4m_\pi^2)^{1.0}}{(t'-t)\sqrt{t'}}\,. \tag{A3}$$

As before, we replace $M_{\pi p}(s,t)$ by $s\sigma_{\pi p} d^{A\bar{t}/2}$ and make the Hankel transform, using Eq. (1) with the Bessel function J_0 replaced by J_n, where $n=1$ is the net helicity flip. Then

$$\tilde{M}_a^{(\frac12-\frac12)}(b) = \frac{g^2\sigma_{\pi p}\exp(A\bar{t}/2)}{256\pi m_c^2} \times \int_{4m_\pi^2} dt\,(t-4m_\pi^2)K_1(b\sqrt{t}\,)\,. \tag{A4}$$

Via the asymptotic form for K_1 and the substitution $t = 4m_\pi^2(1+z)^2$, we obtain

$$\tilde{M}_a^{(\frac12-\frac12)} \simeq \frac{g^2\sigma_{\pi p} m_\pi^4 \exp(A\bar{t}/2)}{32\sqrt{\pi}\, m_c^2} \frac{\exp(-2m_\pi b)}{(m_\pi b)^{5/2}}\,. \tag{A5}$$

This should be a reasonable representation for $b \sim 1-5$ F. The power $b^{-5/2}$ in place of the previous b^{-3} results from approximations. The final asymptotic behavior would not set in until $b \gg 10$ F, and is therefore irrelevant. The ratio of flip to nonflip at $b \simeq 1.5$ F is $\tilde{M}_a^{(\frac{1}{2}-\frac{1}{2})}/\tilde{M}_a^{(\frac{1}{2}\frac{1}{2})} \simeq 0.6$. This agrees reasonably with the result $\simeq 0.7$ obtained by numerical integration, including form factors.

---

*Work supported by the National Science Foundation.

†Work supported by the United States Atomic Energy Commission.

[1]S. Barshay and Y. Chao, Phys. Rev. Lett. 29, 753 (1972); J. Alcock, N. Cottingham, and C. Michael, Nucl. Phys. B67, 445 (1973).

[2]J. Pumplin, F. Henyey, and G. Kane, Phys. Rev. D 10, 2918 (1974).

[3]G. Ascoli *et al.*, Phys. Rev. D 9, 1963 (1974).

[4]F. Henyey, G. Kane, and R. Hong-Tuan, Nucl. Phys. B70, 445 (1974); H. Miettinen (private communication).

[5]J. Pumplin and G. Kane, Phys. Rev. Lett. 32, 963 (1974).

[6]A. Carroll *et al.*, Phys. Rev. Lett. 33, 932 (1974).

[7]N. Samios *et al.*, Rev. Mod. Phys. 46, 49 (1974).

[8]J. Bronzan, G. Kane, and U. Sukhatme, Phys. Lett. 49B, 272 (1974).

[9]While writing this paper, we learned that L. Stodolsky and F. Cho have estimated diffractive A_2 and K^* production by using a Deck model. Our calculation will differ from theirs by a factor of σ_{tot}/σ_{el} in amplitude because we included all inelastic production by π exchange in Fig. 1. Our calculation will also differ in the ratio of helicity-2 to helicity-1 A_2's, because we include absorption effects automatically. The overall phase will probably differ as well, since the Deck model has *two* sides of the triangle diagram [Fig. 1(c)] on the mass shell—see J. Pumplin, Phys. Rev. D 2, 1859 (1970).

[10]Yu. Antipov *et al.*, Nucl. Phys. B63, 153 (1974).